

This is the accepted manuscript made available via CHORUS. The article has been published as:

$R_{\{K\}}$ anomalies and simplified limits on $Z^{\{'\}}$ models at the LHC

R. Sekhar Chivukula, Joshua Isaacson, Kirtimaan A. Mohan, Dipan Sengupta, and
Elizabeth H. Simmons

Phys. Rev. D **96**, 075012 — Published 10 October 2017

DOI: [10.1103/PhysRevD.96.075012](https://doi.org/10.1103/PhysRevD.96.075012)

R_K anomalies and simplified limits on Z' models at the LHC

R. Sekhar Chivukula,^{*} Joshua Isaacson,[†] Kirtimaan A. Mohan,[‡] Dipan Sengupta,[§] and Elizabeth H. Simmons[¶]

*Department of Physics and Astronomy
Michigan State University
567 Wilson Road, East Lansing U.S.A.*

The LHCb collaboration has recently reported a 2.5σ discrepancy with respect to the predicted value in a test of lepton universality in the ratio $R_{K^*} = \text{BR}(B \rightarrow K^* \mu^+ \mu^-) / \text{BR}(B \rightarrow K^* e^+ e^-)$. Coupled with an earlier observation of a similar anomaly in R_K , this has generated significant excitement. A number of new physics scenarios have been proposed to explain the anomaly. In this work we consider simplified limits on Z' models from ATLAS and CMS searches for new resonances in dilepton and dijet modes, and we use the simplified limits variable ζ to correlate the results of the resonance and B-decay experiments. By examining minimal Z' models that can accommodate the observed LHCb results, we show that the high-mass resonance search results are beginning to be sensitive to these models and that future results will be more informative.

I. INTRODUCTION

Run-2 of the LHC is well under way and the hunt for new physics has gathered pace. While no clear signature of physics beyond the standard model (BSM) has been seen yet in the CMS or ATLAS experiments, a large swath of parameter space has been explored in the context of various models. A complementary strategy is explored by the LHCb collaboration (in addition to the experiments Belle, BaBar and KEK), where deviations in B physics observables from predicted standard model values could potentially be a signature of new physics. Over the years, several B -physics processes have shown deviations from Standard model predictions [1]. While there remain certain caveats about state of the art SM calculations, specially in estimating higher order QCD contributions, it is worthwhile to consider new particles that can explain the anomalies and to explore the potential consequences of these particles in other experiments.

Very recently the LHCb experiment has observed an anomaly in a test of lepton flavor universality in the decay $B \rightarrow K^* \ell^+ \ell^-$ with a statistical significance of 2.5σ [2]. Coupled with an earlier observation in the decay $B \rightarrow K \ell^+ \ell^-$, that had a similar anomaly [3], this has generated a significant amount of excitement in the community. A number of studies have already appeared in this context, most of which perform a global fit of the operators that contribute to this anomaly, and quantify the discrepancy in terms of deviations from the corresponding standard model values [4–14]. Some efforts have also been devoted to an explanation with additional gauge bosons (Z'), lepto-quarks, and light particles [15–34]. We also note that similar anomalies have been observed in the measurement of R_D and R_{D^*} and still persist [35].

^{*}Electronic address: sekhar@msu.edu

[†]Electronic address: isaacs21@msu.edu

[‡]Electronic address: kamohan@msu.edu

[§]Electronic address: dipan@msu.edu

[¶]Electronic address: esimmons@msu.edu

While low energy B -physics observables can provide indirect clues to the plausible nature of new physics models, the new particles in these models will have to eventually be directly discovered. Since we have not observed any new particles at the LHC, any explanation of the anomaly has to be consistent with CMS and ATLAS search bounds on such objects. In this paper, we use the simplified limits framework [36], to constrain the parameter space available to a general phenomenological Z' model. On the one hand, we employ this framework for its originally identified purpose of presenting collider data on resonance searches in a form that facilitates identification of production and decay channels that could explain a new excess. On the other, we also show how to use this framework to simultaneously express different pieces of theoretical and experimental information in a unified language that provides an overarching picture of the viable parameter space of the model.

First, we use the R_K and R_{K^*} anomalies to put an upper bound on the value of the “simplified limits variable” ζ ; then, we apply theoretical considerations to obtain a lower bound on ζ . Having identified a swath of parameter space within which a Z' model would be both theoretically self-consistent and able to explain the LHCb observables, we consider how CMS and ATLAS dijet and dilepton data further constrain ζ . We show that high-mass LHC resonance search results are beginning to be sensitive to the general class of Z' models that could be responsible for the R_K and R_{K^*} anomalies – and that future results will be more sensitive.

II. QUANTIFYING THE ANOMALY

As mentioned earlier, there are two independent observations by LHCb that point to lepton flavor violation. The first of them is the ratio [37],

$$R_K = \frac{\text{BR}(B^+ \rightarrow K^+ \mu^+ \mu^-)}{\text{BR}(B^+ \rightarrow K^+ e^+ e^-)} = 0.745 \pm 0.09_{\text{stat}} \pm 0.036_{\text{syst}}; \quad (1)$$

in the bin of $q^2 \in [1, 6] \text{ GeV}^2$. The corresponding predicted SM value is $R_K = 1.0004(8)$ [38]. The second measured anomaly is the recently measured value of R_{K^*} [2],

$$R_{K^*} = \frac{\text{BR}(B \rightarrow K^* \mu^+ \mu^-)}{\text{BR}(B \rightarrow K^* e^+ e^-)}. \quad (2)$$

The measurements in two different dilepton invariant mass squared (q^2) bins using the 1 fb^{-1} data set from LHCb [37] yield,

$$R_{K^*}[0.045, 1.1] \text{ GeV}^2 = 0.660^{+0.110}_{-0.070} \pm 0.024, \quad R_{K^*}[1.1, 6] \text{ GeV}^2 = 0.685^{+0.113}_{-0.069} \pm 0.047. \quad (3)$$

The SM value corresponds to [38, 39]¹,

$$R_{K^*}[0.045, 1.1] \text{ GeV}^2 = 0.920(7), \quad R_{K^*}[1.1, 6] \text{ GeV}^2 = 0.996(2). \quad (4)$$

Individually, each of these measurements point to $\sim 2.5\sigma$ deviations from the standard model predictions.² However, global fits indicate that deviations from the SM are found to be about 4σ [7, 8]. In the past, several analyses have exploited angular distributions in $B \rightarrow K^* \mu^+ \mu^-$ [40–42] to claim that deviations from SM in global fits can be between $4\text{--}5 \sigma$ [43–46]. Yet it has also been observed that hadronic uncertainties can be significant and can bring the significance down considerably [47–60].

¹ Note that the most up to date values of the SM prediction including QED effects, according to [39] are: $R_K[1, 6] \text{ GeV}^2 = 1.00 \pm 0.01$; while $R_{K^*}[0.045, 1.1] \text{ GeV}^2 = 0.901 \pm 0.028$, $R_{K^*}[1.1, 6] \text{ GeV}^2 = 1.00 \pm 0.01$. While this changes the fit values obtained in [8] slightly, the features of this analysis do not change significantly.

² Note that the anomaly in the branching ratio is observed entirely in the muons. The branching ratio to electrons agrees with that of the SM prediction.

The $b \rightarrow sll$ transitions can be studied in the language of effective Lagrangians. To leading order in G_F the effective Hamiltonian for these transitions,³ at low energy in SM, is:

$$\mathcal{H}_{eff}^{SM} = \frac{4G_F}{\sqrt{2}} \sum_{p=u,c} V_{pb} V_{ps}^* \left(C_1 \mathcal{O}_1^p + C_2 \mathcal{O}_2^p + \sum_{i=3}^{10} C_i \mathcal{O}_i \right) \quad (5)$$

The operators that contribute to the effective Hamiltonian can be classified as [8],

- $\mathcal{O}_{1,2}$: Current-current operators.
- $\mathcal{O}_{3,4,5,6}$: QCD penguins.
- \mathcal{O}_7 : Electromagnetic penguin.
- \mathcal{O}_8 : Chromo-magnetic operator.
- $\mathcal{O}_{9,10}$: Semi-leptonic operators.

BSM effects can be studied by modifying Wilson coefficients C_i and by supplementing the Lagrangian with chirally flipped versions of the operators \mathcal{O}_i . It can be shown that the operators $\mathcal{O}_1 \dots \mathcal{O}_8$ do not contribute directly to lepton flavor violation. Out of all the operators described above, the four that can potentially explain the deficits in the measurements of R_K and R_{K^*} are

$$\mathcal{O}_9^{(\prime)} = \frac{\alpha_{em}}{4\pi} (\bar{s}\gamma^\mu P_{L(R)} b) (\bar{l}\gamma_\mu l), \quad \mathcal{O}_{10}^{(\prime)} = \frac{\alpha_{em}}{4\pi} (\bar{s}\gamma^\mu P_{L(R)} b) (\bar{l}\gamma_\mu \gamma_5 l), \quad (6)$$

where the unprimed operators involve left-handed quark currents, the primed ones involve right-handed (chirality-flipped) currents, and P_L, P_R are the left- and right-handed projection operators respectively.

We follow the analysis of [8] to quantify the deviation in terms of non-universal BSM contributions ($\delta C_9, \delta C_{10}$). Although the deficit could arise from a combination of lepton flavor violating effects in both electron and muon sectors, for simplicity we assume that the new physics contribution is muon specific. For the R_K anomaly, since the standard model contribution is $C_9^{SM} \simeq -C_{10}^{SM} = 4.27$, a muon specific BSM contribution requires,

$$\text{either } \delta C_9^{(\prime)\mu} \simeq -1, \quad \text{or } \delta C_{10}^{(\prime)\mu} = +1. \quad (7)$$

Equivalently, one can express the above in terms of a leptonic left handed combination [8],

$$\delta C_9^\mu = -\delta C_{10}^\mu = -0.5. \quad (8)$$

The prediction for the decay width for $\Gamma(B \rightarrow K^* l^+ l^-)$ is more involved. On decomposing the expression for width into a transverse and longitudinal part it can be seen that the longitudinal part of the width differs from $\Gamma(B \rightarrow K l^+ l^-)$ by a relative minus sign in the interference of the SM contribution and its chirally flipped counterpart. This change in sign implies that a simultaneous reduction in both R_K and R_{K^*} cannot be explained by the primed, chirally flipped, operators alone. For instance, a drop in R_K via a negative contribution in the chirally flipped operators would induce an excess in R_{K^*} . In this work we only consider C_9 and C_{10} for simplicity, although this can be extended to a general framework by combining C_9, C_{10} with their chirality flipped counterparts.

Assuming that the anomaly is generated by some new physics (up to possible standard model uncertainties), we will focus on Z' models and look at synergy between LHC constraints and B physics using the language of simplified limits [36].

³ Here and throughout it is understood that the Wilson coefficients and the corresponding matrix elements are renormalized at a scale of order m_b .

III. GENERAL Z' MODEL

Our objective is to use the data from LHCb along with high-energy results from CMS and ATLAS to identify the most compelling limits that can be set on Z' models capable of explaining the R_K and R_{K^*} anomalies. We use the following model-independent parametrization⁴ for the coupling of an extra gauge boson Z' to fermions,

$$\begin{aligned} \mathcal{L}_{Z'} = & \frac{1}{4} F^{\mu\nu} F_{\mu\nu} + \frac{1}{2} m_{Z'}^2 Z'^\mu Z'_\mu \\ & + \beta_{Z'} Z'_\mu \sum_{f=u,c,t} \sum_{\bar{f}=u,c,t} (c_L^{f'\bar{f}} \bar{f}' \gamma^\mu P_L f + c_R^{f'\bar{f}} \bar{f}' \gamma^\mu P_R f) \\ & + \beta_{Z'} Z'_\mu \sum_{f=d,s,b} \sum_{\bar{f}=d,s,b} (c_L^{f'\bar{f}} \bar{f}' \gamma^\mu P_L f + c_R^{f'\bar{f}} \bar{f}' \gamma^\mu P_R f) \\ & + \beta_{Z'} Z'_\mu \sum_{f=\text{leptons}} (c_V^f \bar{f} \gamma^\mu f + c_A^f \bar{f} \gamma^\mu \gamma_5 f) , \end{aligned} \quad (9)$$

where f, \bar{f} are SM fermions. The above parametrization therefore contains chiral couplings to quarks (c_L, c_R), and vector and axial vector couplings (c_V, c_A) to leptons. Motivated by the LHCb results, we allow for flavor-changing neutral-currents in the quark sector and ignore them in the leptonic sector. Finally, we use the normalization

$$\beta_{Z'} = m_{Z'} \sqrt{\frac{\alpha_{em} V_{tb} V_{ts}^*}{2\pi v^2}} , \quad (10)$$

so that (ignoring renormalization effects between the scales $M_{Z'}$ and m_b) the Wilson coefficients of the effective Lagrangian are related to the parameters of the Z' Lagrangian as follows,

$$C_9^\mu \simeq c_L^{sb} c_V^\mu , \quad C_{10}^\mu \simeq c_L^{sb} c_A^\mu , \quad (11)$$

$$C_9'^\mu \simeq c_R^{sb} c_V^\mu , \quad C_{10}'^\mu \simeq c_R^{sb} c_A^\mu . \quad (12)$$

In the above, we have taken $V_{tb} = 1$ and $V_{ts} = 0.040$. One can invert these four equations and solve for $c_{L,R,V,A}$. Note, however, that in order to obtain a unique solution, one needs at least three of the Wilson coefficients to be non-zero. Furthermore, in order to explain the anomaly with a single Z' , we see that

$$\frac{C_9^\mu}{C_9'^\mu} = \frac{C_{10}^\mu}{C_{10}'^\mu} , \quad (13)$$

The analysis above sets constraints on predictions of any underlying model with a Z' . While the Z' must, at a minimum, couple to the bottom and the strange quark and decay to leptons to explain the anomaly, in a realistic model the Z' can couple to the light quarks (and possibly the top) as well. However, note that Eq. 13 implies that the value of c_L^{sb} is not uniquely fixed by the best fit values of C_9 and C_{10} . As we will show below, the value of c_L^{sb} determines the overall strength of the Z' signal at the LHC in this minimal phenomenological model.

In the next sections, we will explore the constraints on our Z' model arising from the LHCb observations, several theoretical considerations, and the dijet and dilepton searches for new resonances that are being conducted by the ATLAS and CMS collaborations. We will use the language of simplified limits [36] as a way to simultaneously express these different pieces of information and gain an overarching picture of the viable parameter space of the model. First we will briefly review the key aspects of the simplified limits framework. Then we will explore constraints on the simplest version of our Z' model, in which its coupling to quarks comes only through a flavor-changing coupling to sb . Following that, we see how the constraints are impacted if the Z' also has a flavor-conserving coupling to quarks.

⁴ Here, following a simplified model analysis, for simplicity we ignore flavor-changing neutral-currents (FCNC) in the leptonic sector and do not consider neutrino couplings. As noted by the authors in [24], however, these constraints are likely to be important in any complete theory.

IV. SIMPLIFIED LIMITS IN THE NARROW WIDTH APPROXIMATION

Here, we will briefly review the simplified limits framework that was introduced in [36] as a way to quickly understand how observing a new resonance in a particular production and decay channel could restrict the types of models available to explain the observation. As discussed below, this framework will be useful for comparing several different kinds of information about our Z' model, ranging from collider search data to the LHCb observations to various theoretical bounds.

We will assume that the observed new resonance is narrow, such that any interference of standard model and new physics contributions can be neglected. Thus the tree level partonic cross section for an s channel narrow resonance R , decaying to a final state(s) $x + y$ from initial state partons $i + j$ can be written as,

$$\hat{\sigma}_{ij \rightarrow xy} = 16\pi(1 + \delta_{ij}) \frac{N_{S_R}}{N_{S_i} N_{S_j}} \frac{C_R}{C_i C_j} \Gamma(R \rightarrow x + y) \Gamma(R \rightarrow i + j) \frac{\pi}{m_R \Gamma_R} \delta(\hat{s} - m_R^2). \quad (14)$$

In the above equation N_S and C count the number of spins and colors for the resonance R and the incoming partons i and j . The total cross section can be obtained by integrating the partonic cross section over parton luminosities, and summing over incoming partons that contribute (*e.g.*, light quarks = u, d, c, s) and outgoing final states defining the signature of interest (*e.g.* light quarks for dijets, or e and μ for dileptons),

$$\sigma = 16\pi^2 \frac{N_{S_R}}{N_{S_i} N_{S_j}} \frac{C_R}{C_i C_j} \frac{\Gamma_R}{m_R} \times \left(\sum_{ij} (1 + \delta_{ij}) BR(R \rightarrow i + j) \left[\frac{1}{s} \frac{dL_{ij}}{d\tau} \right]_{\tau=\frac{m_R^2}{s}} \right) \left(\sum_{xy} \Gamma(R \rightarrow x + y) \right), \quad (15)$$

where the luminosity function $\frac{dL_{ij}}{d\tau}$ is given by,⁵

$$\frac{dL_{ij}}{d\tau} = \frac{1}{1 + \delta_{ij}} \int_{\tau}^1 \frac{dx}{x} \left[f_i(x, \mu_F^2) f_j\left(\frac{\tau}{x}, \mu_F^2\right) + f_j(x, \mu_F^2) f_i\left(\frac{\tau}{x}, \mu_F^2\right) \right]. \quad (16)$$

It is useful to define the dimensionless “simplified limits variable”, ζ ,

$$\zeta \equiv \frac{\Gamma}{m_{Z'}} \sum_{production} (1 + \delta_{ij}) BR(Z' \rightarrow i + j) \sum_{decay} BR(Z' \rightarrow x + y), \quad (17)$$

which, as described more fully in [36], is a convenient general variable for expressing search limits for narrow resonances. This variable is defined with respect to each production and decay channel and is related to the effective size of the resonance-signal in that channel.

In prior work, we showed how to use ζ as a tool for efficiently relating an observed signal of new physics to the predictions of entire classes of models at once. Here, we will use ζ as a common variable via which disparate constraints on a model may be compared. We will both identify the range of ζ values our Z' model must exhibit in order to explain the LHCb observations and analyze whether new particle searches at the ATLAS and CMS experiments are sensitive to that range of ζ values. This will enable us to see whether our Z' model remains viable in light of recent collider searches.

The form of the simplified limits variable for our Z' boson in the dimuon decay channel may be obtained⁶ by applying Eqs. 9 and 10 to Eq. 17:

$$\zeta^\mu = \left(\sum_{f, f' = quarks} \frac{\beta_{Z'}^2 (|c_L^{f'f}|^2 + |c_R^{f'f}|^2)}{4\pi} \right) \left(\frac{(|c_A^\mu|^2 + |c_V^\mu|^2)}{3 \sum_{quarks} |c_i^{ff'}|^2 + \sum_{leptons} |c_i^j|^2} \right). \quad (18)$$

⁵ In this paper, for the purposes of illustration, we calculate these parton luminosities using the CT14NLO [61] parton density functions, setting the factorization scale $\mu_F^2 = m_R^2$.

⁶ As explained in [36], to interpret this ratio correctly one must also account for the different possible incoming partonic production mechanisms.

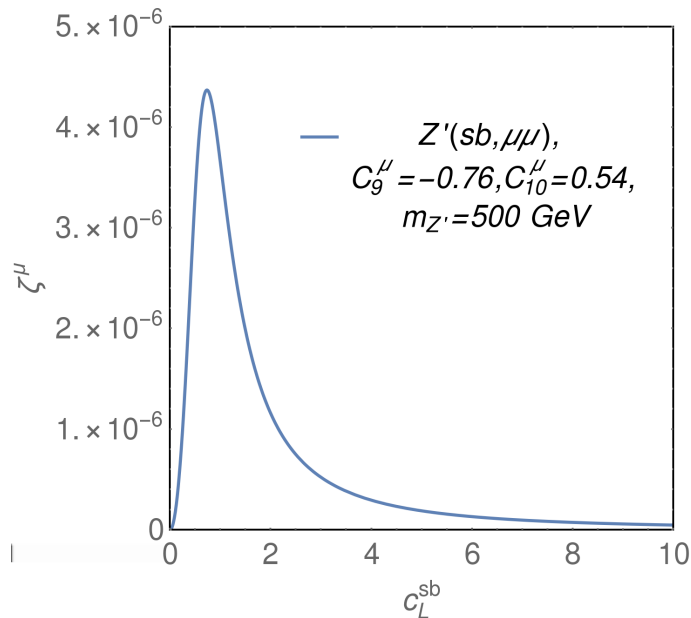


FIG. 1: The simplified limits variable ζ^μ as a function of c_L^{sb} , for a Z' coupling only to sb and muons; shown for the best fit values of C_9, C_{10} . The mass of the Z' only affects the normalization of this curve. The upper and lower bounds on $|c_L^{sb}|$ arise from requiring the Z' couplings to remain perturbative. Note that the lowest value of ζ^μ occurs for the smallest allowed value of c_L^{sb} .

In the denominator of the second factor, the subscript i runs over left and right handed contributions for quarks, and over vector and axial vector contributions from leptons. A similar expression, ζ^j for the dijet signature, is easily found by replacing the numerator in the last factor by a sum over the relevant light-quark couplings. Thus ζ^μ is quadratic in the undetermined parameter c_L , while ζ^j is quartic in c_L .

In the next two sections we use this formalism to assess the R_K anomaly in light of theoretical considerations and also the CMS and ATLAS data gathered at 8 and 13 TeV.⁷

V. CONSTRAINTS ON A Z' COUPLING ONLY TO sb AND $\mu\mu$

We now consider how a Z' -model that accomodates the R_K anomalies would be constrained by theoretical information and by searches for dilepton and dijet resonances at ATLAS and CMS. For the purpose of illustration, we will evaluate ζ^μ using representative Wilson coefficient values of ($C_9^\mu = -0.76, C_{10}^\mu = 0.54, C_9^{\prime\mu} = 0, C_{10}^{\prime\mu} = 0$) that are derived from fits performed using low energy data [8].⁸

Let us first consider a phenomenological model where the Z' couples to quarks only through the off-diagonal sb coupling and also couples to muons but not other leptons. This limiting case satisfies the minimum requirements in order for the Z' to explain the R_K anomalies and, as we will see, yields a wide range of allowable parameter space. We will consider the more realistic case of a Z' with flavor-diagonal couplings to quarks, as well as the necessary sb coupling, in Section VI.⁹

⁷ An analysis constraining 36 four fermion operators using dilepton data in the high p_T tail was performed in [62].

⁸ While different groups obtain larger significances depending on the fit parameters, we chose the more conservative estimates of these Wilson coefficients [8].

⁹ Having only off-diagonal sb couplings, especially left-handed ones, would require very specific choices for the gauge-couplings and for

A. Upper limit on ζ^μ

In the limiting case under consideration, the Z' is produced at the LHC only through $\bar{b}s + \bar{s}b$ luminosities. Henceforth, we will use the shorthand notation qq' to mean $(\bar{q}q' + \bar{q}'q)$. Under these assumptions, the form of ζ^μ shown in Eq. 18 reduces to

$$\begin{aligned}\zeta^\mu &= \beta_{Z'}^2 \frac{(c_L^{sb})^2}{4\pi} \left(\frac{(|c_A^\mu|^2 + |c_V^\mu|^2)}{3|c_L^{sb}|^2 + (|c_A^\mu|^2 + |c_V^\mu|^2)} \right) \\ &= \beta_{Z'}^2 \frac{(c_L^{sb})^2}{4\pi} \left(\frac{(C_9^\mu)^2 + (C_{10}^\mu)^2}{3|c_L^{sb}|^4 + ((C_9^\mu)^2 + (C_{10}^\mu)^2)} \right).\end{aligned}\quad (19)$$

We present the relationship between ζ^μ and c_L^{sb} in Fig. 1 for $m_{Z'} = 500$ GeV, and setting C_9, C_{10} at their best fit values. The only effect the mass has on the curve is to change the normalization of the y -axis.

The curve in Fig. 1 shows that ζ^μ has a maximum with respect to c_L^{sb} ; extremizing the expression for ζ^μ in Eq. 19 identifies the value of c_L^{sb} where the maximum occurs as

$$c_L^{sb} = \left\{ \frac{1}{3} ((C_9^\mu)^2 + (C_{10}^\mu)^2) \right\}^{1/4} \simeq 0.73. \quad (20)$$

Using this value in Eq. 19 reveals an upper bound on ζ given by,

$$\zeta_{max}^\mu = \beta_{Z'}^2 \frac{\left\{ \frac{1}{3} ((C_9^\mu)^2 + (C_{10}^\mu)^2) \right\}^{1/2}}{8\pi}. \quad (21)$$

The value of ζ_{max}^μ determines the maximum possible size of the dimuon signal that our Z' could produce at ATLAS and CMS. To see this, compare Eqs. 15 and 17; one can clearly write ζ^μ in terms of the size of the peak cross-section for producing the resonance. As described in detail in [36], the precise relationship is:

$$\zeta = \frac{\sigma}{16\pi^2 \cdot \frac{N_{S_R}}{N_{S_i} N_{S_j}} \times \left[\sum_{ij} \omega_{ij} \left[\frac{1}{s} \frac{dL^{ij}}{d\tau} \right]_{\tau = \frac{m_R^2}{s}} \right]}. \quad (22)$$

where the weighting factor ω is defined as

$$\omega_{ij} \equiv \frac{(1 + \delta_{ij}) BR(R \rightarrow i + j)}{\sum_{i'j'} (1 + \delta_{i'j'}) BR(R \rightarrow i' + j')}. \quad (23)$$

Since the parton luminosities and the spin and color factors are fixed, the maximum ζ^μ does indeed correspond to a maximum value of σ .

B. Lower limit on ζ^μ from Perturbativity

Retaining our present focus on a Z' with only off-diagonal coupling to quarks, the minimum size of ζ^μ that is consistent with the LHCb observations is determined by several theoretical considerations. The first constraint we assess is that of perturbativity of this phenomenological Z' model.

Perturbativity requires that all quark and lepton couplings be bounded from above. Based on the notation in Eq. 9, we will use the estimates:

$$\beta'_Z \times |c_L^{sb}| < 4\pi \quad \text{and} \quad \beta'_Z \times |c_V^\mu| < 4\pi \quad (24)$$

the rotations required to translate between the gauge-eigenstate and mass-eigenstate bases for the light fermions. As we will see, having additional flavor-diagonal couplings to light quarks will generally enhance the dilepton and diquark signatures for the Z' , and will correspondingly reduce the parameter space by current experimental constraints.

to establish the conditions under which perturbativity exists. The first of these tells us directly that $|c_L^{sb}| < 4\pi/\beta_{Z'}$. To interpret the second, we note that from Eq. 11 we can write,

$$c_V^\mu = \frac{C_9}{c_L^{sb}}, \quad c_A^\mu = \frac{C_{10}}{c_L^{sb}}. \quad (25)$$

Therefore, from the benchmark value of C_9 , we can derive a lower limit¹⁰ on the value of $|c_L^{sb}|$ to pair with the upper limit mentioned just above:

$$\frac{0.76\beta_{Z'}}{4\pi} < |c_L^{sb}| < \frac{4\pi}{\beta_{Z'}} \quad (26)$$

Incorporating information from Eq. 10, we find

$$1.73 \times 10^{-6} [\text{GeV}]^{-1} m_{Z'} < |c_L^{sb}| < \frac{4.4 \times 10^5 [\text{GeV}]}{m_{Z'}}. \quad (27)$$

Note that the allowed range of values of $|c_L^{sb}|$ reduces in scope with increasing $m_{Z'}$.

As may be seen from the shape of the curve plotted in Fig. 1, for a given mass $m_{Z'}$ the lower bound on c_L^{sb} that we have just derived yields a *lower bound* on ζ^μ , which we will denote ζ_{pert}^μ .

Finally, we note that the flavor changing neutral currents mediated by the Z' affect the $B_s^0 - \bar{B}_s^0$ system and contribute to mixing of the states through a tree level diagram. It is possible to use the measured mass difference in the $B_s^0 - \bar{B}_s^0$ system to determine an upper bound on c_L^{sb} ¹¹. We find that $|c_L^{sb}| \lesssim 4.4 \times 10^4$ at 95% confidence level. For resonances with masses in the TeV range, as considered here, this limit is much weaker than the upper bound derived above from perturbativity arguments.

C. Lower limit on ζ^μ Due to the Z' Width

For a Z' boson coupling only to the s , b and μ , the expression for the decay width is,

$$\Gamma = \beta_{Z'}^2 \left[\frac{1}{12\pi} \left(\frac{(C_{10}^\mu)^2}{(c_L^{sb})^2} + \frac{(C_9^\mu)^2}{(c_L^{sb})^2} \right) + \frac{(c_L^{sb})^2}{4\pi} \right] m_{Z'} \quad (28)$$

As noted earlier, we will focus on narrow resonances, defined as those satisfying $\Gamma/M \leq \alpha_{max}$ for a value of α_{max} that we will specify below. Restricting our attention to narrow resonances provides constraints on the value of c_L^{sb} given by,

$$\frac{4\pi\alpha_{max}}{2\beta_{Z'}^2} (1 - \sqrt{D}) < (c_L^{sb})^2 < \frac{4\pi\alpha_{max}}{2\beta_{Z'}^2} (1 + \sqrt{D}) \quad (29)$$

where the discriminant D is defined as

$$D \equiv \left[1 - \frac{\beta_{Z'}^4}{12\pi^2(\alpha_{max})^2} \cdot ((C_{10}^\mu)^2 + (C_9^\mu)^2) \right] \quad (30)$$

with $\Gamma/m_{Z'} = \alpha_{max}$. Values of c_L^{sb} falling below the lower bound, though potentially consistent with the perturbativity constraint in Eq. 26, would nonetheless yield $\Gamma/M > \alpha_{max}$. So this provides a stricter lower bound on c_L^{sb} . We will denote the value of ζ^μ corresponding to this lowest value of c_L^{sb} by the symbol ζ_{narrow}^μ .

¹⁰ For our benchmark values, the smaller magnitude of C_{10} would yield a weaker constraint.

¹¹ For a description of the details of this calculation, see for example ref [63]

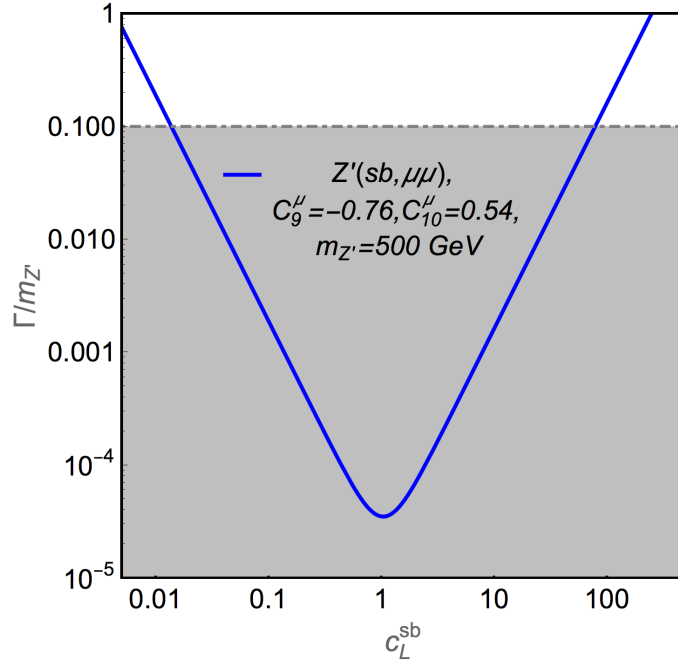


FIG. 2: Dependence of $\Gamma/m_{Z'}$ upon c_L^{sb} . The shaded region corresponds to Z' boson with a narrow width, $\Gamma/M < 0.1$.

Fig. 2 displays the dependence of $\Gamma/m_{Z'}$ on c_L^{sb} . The shaded region corresponds to the values of c_L^{sb} where the Z' has a narrow width, which we hereafter specifically take to mean $\Gamma/M < \alpha_{max} = 0.1$. In addition to the minimum value of c_L^{sb} for which the Z' boson is still “narrow”, we can also identify in the figure a unique value of c_L^{sb} at which Γ/M is minimized. Comparing Eqs. 19 and 28 shows that for fixed $C_{9,10}$ the width is inversely proportional to ζ^μ , so that the value of c_L^{sb} at which Γ/M is minimized also corresponds to ζ_{max}^μ in Eq. 20.

Furthermore, since the resonance width in Eq. 28 is proportional to the cube of the mass, the solid curve in Fig. 2 moves upward as the mass of the Z' increases (assuming fixed values of C_9^μ and C_{10}^μ). For a heavy enough Z' , only the lowest point of the solid curve will still be within the shaded region; i.e., only for that unique value of c_L^{sb} will the resonance still be narrow. This happens when the discriminant D becomes negative, which allows us to find the corresponding maximum value of the Z' mass (shown for $\alpha_{max} = 0.1$).

$$m_{Z'} < \sqrt{\frac{4\sqrt{3}\pi^2 v^2 \alpha_{max}}{((C_{10}^\mu)^2 + (C_9^\mu)^2)^{1/2} \alpha_{em} V_{tb} V_{ts}^*}} \simeq 37.8 \text{ TeV} . \quad (31)$$

The interesting range of the simplified limits variable ζ^μ for this minimal model where the Z' boson couples only to s , b , and μ is therefore $\zeta_{pert,narrow}^\mu < \zeta^\mu < \zeta_{max}^\mu$. We will now consider what the ATLAS and CMS resonance searches in the dilepton and dijet channels can say about that region of parameter space.

D. Upper limit on ζ^μ from dilepton resonance searches.

The ATLAS and CMS experiments are searching for new resonances decaying to dileptons, and therefore can potentially constrain or discover the Z' boson proposed here. As discussed in [36], the simplified limits variable ζ^μ provides a useful way to report the results of such searches. Here, we will find that it also enables us to overlay several different kinds of information about our Z' state.

We use both 8 TeV and 13 TeV dilepton resonance searches at the LHC to extract limits on the model [64, 65].

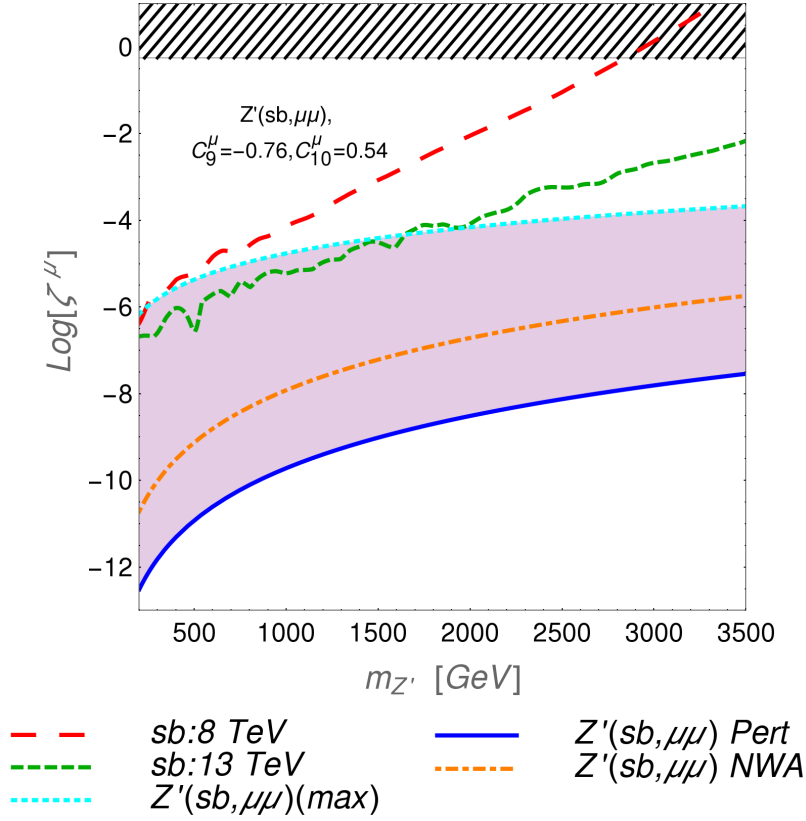


FIG. 3: Constraints on the Z' coupling only to s , b , and μ . The pink shaded region shows where ζ^μ is small enough (below light-blue dashed line) to explain the R_K and R_{K^*} anomalies and also large enough (above blue solid line) to keep the Z' boson's couplings perturbative. Above the orange dot-dashed line, the Z' would be narrow. The maximum upper bounds (from the absence of observing dilepton resonances) on ζ^μ derived from both the 8 TeV (red long-dashed) and 13 TeV (green dashed) ATLAS dilepton limits [64–66] are shown for comparison. We see that LHC dilepton results are only beginning to be sensitive to the region which can explain the R_K anomalies.

Specifically, we use Eq. 22 to reframe the experimental limits on $\sigma \cdot B \cdot \mathcal{A}$ as upper bounds on ζ^μ , following the methods of [36]. Fig. 3 displays the resulting constraints in the $\log \zeta^\mu - m_{Z'}$ plane. The red long-dashed line corresponds to the upper limit on the value of ζ^μ from dilepton constraints assuming sb -initiated production at 8 TeV, while the green dashed line shows how that bound is strengthened by the data taken at 13 TeV.

The pink shaded curved band represents the region of ζ^μ values that simultaneously explain the R_K anomalies (i.e., fall below the light-blue dotted line) and remain consistent with perturbativity (i.e., lie above the solid blue curve). Points lying above the orange dot-dashed line within the shaded band correspond to cases where the Z' resonance is narrow.

At present, the LHC dilepton resonance searches leave this allowed region of $\zeta^\mu - m_{Z'}$ space essentially intact for Z' boson that couples only to s , b , and μ . The 8 TeV data provides an upper bound on ζ^μ for Z' masses below 300 GeV. The 13 TeV data, however, is able to probe further into the upper edge of the pink band for a Z' mass below 1.7 TeV, and excludes some of those values of ζ^μ . We anticipate that future LHC dilepton data will explore the region defined by the pink band more thoroughly, thereby testing our Z' model's viability as an explanation of the R_K anomalies.

In principle, one can also use dilepton data to extract the flavor non-universality limits by comparing the cross-sections in the di-electron channel versus the di-muon channel [67] in the high mass Drell-Yan data. Using the narrow width approximation, as described above, the interference of the Z' with the Drell-Yan background can be neglected.

Therefore, the predicted flavor cross-section ratio is given by:

$$\frac{\sigma(pp \rightarrow \mu^+\mu^-)}{\sigma(pp \rightarrow e^+e^-)} = 1 + \frac{\sigma_{Z'}}{\sigma_{\text{SM}}}. \quad (32)$$

Due to a lack of information about the uncertainties of this measurement, however, we do not use the existing data to impose a limit on the Z' model via this method. We expect this will become a valuable line of inquiry as future data emerges.

E. Upper limit on ζ^j from dijet resonance searches.

Searches for new physics in dijet final states have been conducted by the ATLAS and CMS collaborations [68–70]. In this section we will show the relation between the constraints derived from dijet resonance searches and those from the dilepton resonance searches discussed earlier.

Following the reasoning used to define ζ^μ for the process $sb \rightarrow Z' \rightarrow \mu\mu$, we can analogously define the variable ζ^j for $sb \rightarrow Z' \rightarrow jj$:

$$\begin{aligned} \zeta^j &= \beta_{Z'}^2 \frac{3(c_L^{sb})^4}{4\pi} \left(\frac{1}{3|c_L^{sb}|^2 + (|c_A^\mu|^2 + |c_V^\mu|^2)} \right) \\ &= \beta_{Z'}^2 \frac{3(c_L^{sb})^6}{4\pi} \left(\frac{1}{3|c_L^{sb}|^4 + (|C_9^\mu|^2 + |C_{10}^\mu|^2)} \right) \end{aligned} \quad (33)$$

Note that ζ^j is a monotonically increasing function of c_L^{sb} ; hence there is no equivalent for ζ^j of the lower bound we found for ζ^μ based on maintaining perturbativity of the Z' boson's couplings to fermions or narrowness of the resonance's width. Moreover, even though ζ^μ is generally double-valued in c_L^{sb} , its maximum value, ζ_{max}^μ , corresponds to a unique value of c_L^{sb} (as in Fig. 1 and Eq. 20); it therefore corresponds to a unique value of ζ^j through the formal relationship $\zeta^j = 3\zeta^\mu(c_L^{sb})^4/(|C_9^\mu|^2 + |C_{10}^\mu|^2)$ that is implied by Eqs. 19 and 33. We will use this in relating the various collider limits to one another.

In Fig. 4 the blue (dot-dashed) line shows the upper bound on ζ^j imposed by dijet resonance searches using 36 fb^{-1} of CMS data at a center of mass energy of 13 TeV [68].¹² The green (dashed) line shows the value of ζ^j corresponding to ζ_{max}^μ . The horizontally hatched area at the left edge shows the region of ζ^j and M_R that are ruled out by the dilepton resonance searches discussed earlier. As shown in Fig. 1, each value of ζ^μ (except ζ_{max}^μ) corresponds to two different values of c_L^{sb} . Therefore, as the ATLAS data impose an upper bound on ζ^μ , some intermediate range of c_L^{sb} values is eliminated, leaving both smaller and larger values of c_L^{sb} still allowed. As ζ^j is a monotonically increasing function of c_L^{sb} , this results in eliminating a range of ζ^j values to either side of the ζ_{max}^μ curve in Fig. 4. The hatched region stops abruptly at about 1.7 TeV because, as shown in Fig. 3, the dilepton experimental constraints on ζ^μ only are only sensitive to the theoretically interesting range of ζ^μ for Z' bosons with masses below that value.

VI. CONSTRAINTS ON A Z' COUPLING TO ALL FERMIONS

So far we have considered the case when the Z' couples only to strange quarks, bottom quarks, and muons. We now generalize the constraints discussed above to the situation when the Z' couples to all fermions.¹³

¹² Note that the dijet and dilepton bounds are exclusions at 95 % C.L. (2σ).

¹³ Generically, we see from Eq. 17 that the addition of bosonic decay channels will reduce the value of ζ^j , weakening somewhat the limits discussed below. Qualitatively, however, the features described here remain unchanged.

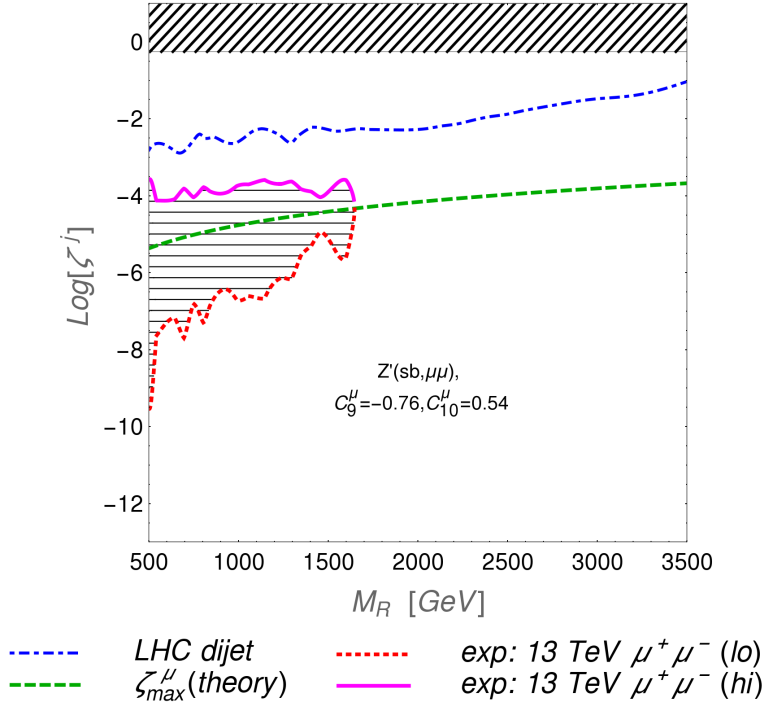


FIG. 4: Constraints on the Z' model in the $\log \zeta^j$ vs mass plane. The blue (dot-dashed) line is the maximum allowed upper bound on ζ^j from the absence of observed dijet resonances by CMS at 13 TeV energy [68]. The green (dashed) line indicates the value of ζ^j corresponding to ζ_{max}^μ , associated with a unique value of c_L^{sb} . Both higher and lower values of ζ^j are allowed by moving away from that specific value of c_L^{sb} . The horizontally hatched region on the left edge indicates values of ζ^j that are ruled out by dilepton searches as consistent with our benchmark values of C_9^μ and C_{10}^μ .

To make our discussion more tractable, we define a simplified notation as follows:

$$c_q^2 \equiv \frac{1}{2} \sum_{f=u,d,s,c,b} \left(|c_L^{ff}|^2 + |c_R^{ff}|^2 \right) + \sum_{ff'=\{uc,ds,db\}} \left(|c_L^{ff'}|^2 + |c_R^{ff'}|^2 \right), \quad (34)$$

$$c_t^2 \equiv \frac{1}{2} \sum_{f=t} \left(|c_L^{ff}|^2 + |c_R^{ff}|^2 \right) + \sum_{ff'=\{ut,ct\}} \left(|c_L^{ff'}|^2 + |c_R^{ff'}|^2 \right). \quad (35)$$

Thus c_q corresponds to all possible partonic combinations in pp collisions¹⁴. We also define,

$$c_e^2 \equiv |c_V^e|^2 + |c_A^e|^2 \quad (36)$$

$$c_\tau^2 \equiv |c_V^\tau|^2 + |c_A^\tau|^2 \quad (37)$$

$$c_\mu^2 \equiv |c_V^\mu|^2 + |c_A^\mu|^2 = \frac{((C_9^\mu)^2 + (C_{10}^\mu)^2)}{|c_L^{sb}|^2} + \frac{((C_9'^\mu)^2 + (C_{10}'^\mu)^2)}{|c_R^{sb}|^2} \quad (38)$$

For the ease of discussion we again set $C_9'^\mu = C_{10}'^\mu = 0$, so that $c_R^{sb} = 0$. Additionally, we also set $c_e = 0$, and choose

¹⁴ We neglect the top quark pdfs inside the proton. We also ignore top mass effects in the decay width for the time being to simplify our discussion.

non-zero values only for c_τ and c_q . With the above assumptions ζ^μ is given by,

$$\begin{aligned}\zeta^\mu &= \left(\sum \frac{\beta_{Z'}^2 (|c_L^{f'f}|^2 + |c_R^{f'f}|^2)}{4\pi} \right) \left(\frac{(|c_A^\mu|^2 + |c_V^\mu|^2)}{3 \sum_{quarks} |c_i^j|^2 + \sum_{leptons} |c_i^j|^2} \right) \\ &= \frac{\beta_{Z'}^2}{4\pi} (c_q^2 + (c_L^{sb})^2) \frac{(c_\mu^2)}{3c_q^2 + 3(c_L^{sb})^2 + c_\mu^2 + c_\tau^2}.\end{aligned}\quad (39)$$

The maximum value of ζ^μ now corresponds to the following value of c_L^{sb} :

$$c_L^{sb} = \left(\frac{\sqrt{(C_{10}^\mu)^2 + (C_9^\mu)^2 - c_\tau^2 c_q^2}}{\sqrt{3}} - c_q^2 \right)^{1/2}.\quad (40)$$

Since ζ^μ is a real quantity, we observe that its maximum allowed value corresponds to $c_L^{sb} = 0$ in two situations: either when $c_\tau^2 c_q^2 > (C_{10}^\mu)^2 + (C_9^\mu)^2$, or when $\frac{\sqrt{(C_{10}^\mu)^2 + (C_9^\mu)^2 - c_\tau^2 c_q^2}}{\sqrt{3}} < c_q^2$.

A. Upper limit on ζ^μ

By applying Eqs. 38 and 40 to Eq. 39, we obtain a general expression for the maximum value of ζ^μ

$$\zeta_{max}^\mu = \frac{\beta_{Z'}^2 ((C_{10}^\mu)^2 + (C_9^\mu)^2)}{4\pi \left(2\sqrt{3} \sqrt{((C_{10}^\mu)^2 + (C_9^\mu)^2 - c_\tau^2 c_q^2)} + 4c_\tau^2 - 3c_q^2 \right)}.\quad (41)$$

From this equation, we see that introducing only c_τ (and setting $c_q = 0$), reduces the maximum value of ζ ; i.e., adding decay modes that do not contribute to Z' production reduces ζ_{max}^μ . Conversely, if we set $c_\tau = 0$ then allowing $c_q \neq 0$ increases the maximum value of ζ^μ ; adding decay modes that contribute to production (beyond the minimum required production via sb annihilation) increases the value of ζ_{max}^μ . Keep in mind, however, that if $((C_{10}^\mu)^2 + (C_9^\mu)^2) < c_\tau^2 c_q^2$, then $c_L^{sb} = 0$, and without the flavor-diagonal coupling to quarks, our Z' boson would not be able to explain the R_K anomalies.

B. Lower limit on ζ^μ from Perturbativity

While the perturbativity constraints on c_L^{sb} itself remain unchanged, the expression for the minimum value of ζ^μ that is allowed by perturbativity is altered. The general form of ζ^μ can now be written as,

$$\zeta^\mu = \frac{\beta_{Z'}^2 (C_{10}^2 + C_9^2) ((c_L^{sb})^2 + c_q^2)}{4\pi (C_{10}^2 + C_9^2 + (c_L^{sb})^2 (c_\tau^2 + 3((c_L^{sb})^2 + c_q^2)))}.\quad (42)$$

Comparing this with the form of Eq. 19 shows that the constraint on perturbativity is weaker than in the situation where the Z' couples only to bottom and strange quarks.

C. Lower limit on ζ^μ Due to the Z' Width

For the generalized scenario the decay width is given by,¹⁵

$$\Gamma = \beta_{Z'}^2 \left[\frac{1}{12\pi} \left(\frac{(C_{10}^\mu)^2}{(c_L^{sb})^2} + \frac{(C_9^\mu)^2}{(c_L^{sb})^2} + c_\tau^2 \right) + \frac{(c_L^{sb})^2 + c_q^2 + c_t^2}{4\pi} \right] m_{Z'} \quad (43)$$

Comparing this with Eq. 28, indicates that the resulting constraint on ζ^μ will be stronger than was the case for the Z' boson coupling only to s , b and μ .

D. Upper limit on ζ^μ from dilepton resonance searches.

The ATLAS dilepton resonance searches at 13 TeV [64–66] give rise to upper bounds on ζ^μ as described earlier; our results for the Z' coupling to all fermions appear in Fig. 5. The location and shape of each limit curve in the $\log[\zeta^\mu] - m_{Z'}$ plane depend on one's assumptions about the dominant production mechanism for the Z' state. We capture the range of possibilities by showing a curve that assumes the Z' is primarily produced by $b\bar{b}$ annihilation (which gives a relatively weak constraint due to the smaller parton luminosity involved) and another assuming that production via $u\bar{u}$ dominates. The horizontally-hatched region between these curves is the region within which the upper bound on ζ^μ for any Z' boson coupling to a combination of $b\bar{b}$ and $u\bar{u}$ will fall. For comparison, we also show the curve assuming that the Z' is produced only through an off-diagonal sb coupling.

Fig. 5 also shows, as a pink band, the swath of parameter space of greatest interest for our simplest model. The upper border (light-blue dotted line) delineates the area that can explain the R_K anomalies; there is an absolute lower limit originating from perturbativity (blue-solid line), and a comparatively softer constraint if we demand that the resonance is narrow (orange dashed) line. For this Z' boson coupling to all fermion flavors, the dilepton search limits are potentially able to rule out a significant fraction of the parameter space that can explain the R_K anomalies.

Note, however, that the precise location and size of the pink band in the general model will vary depending on which additional Z' production and decay modes become available. Relative to the top of the pink band from the minimal case that is reproduced in Fig. 5, the upper edge denoting the upper limit on ζ^μ moves down (up) when additional production (decay) modes are included in the model. The location of the bottom edge of the pink band (from perturbativity constraints) moves down when any additional modes are added, thereby increasing the size of the pink band. The location of the orange dashed line (denoting a narrow resonance) always moves upwards relative to what is shown in Fig. 5, giving rise to stronger constraints; details depend on how many additional non-zero couplings are present.

Searches for new resonances decaying to dijets yield constraints on ζ^j similar to those illustrated in Fig. 4, along the lines discussed in Sec. V E. The precise regions allowed or ruled out depend on the dominant Z' production mechanism – and bounds similar to those shown in Fig. 4 can be derived separately for each production mode.

VII. SUMMARY OF CONSTRAINTS

The summary of all constraints is presented in Figs. 3, 5 and Fig. 4 in the $\log[\zeta^\mu]$ vs $M_{Z'}$ and $\log[\zeta^j]$ vs $M_{Z'}$ plane respectively, for the illustrative values of C_9^μ and C_{10}^μ chosen. We note that for both the minimal and the general cases, the constraints are similar in nature:

¹⁵ Expressions for the partial widths are given in Appendix A.

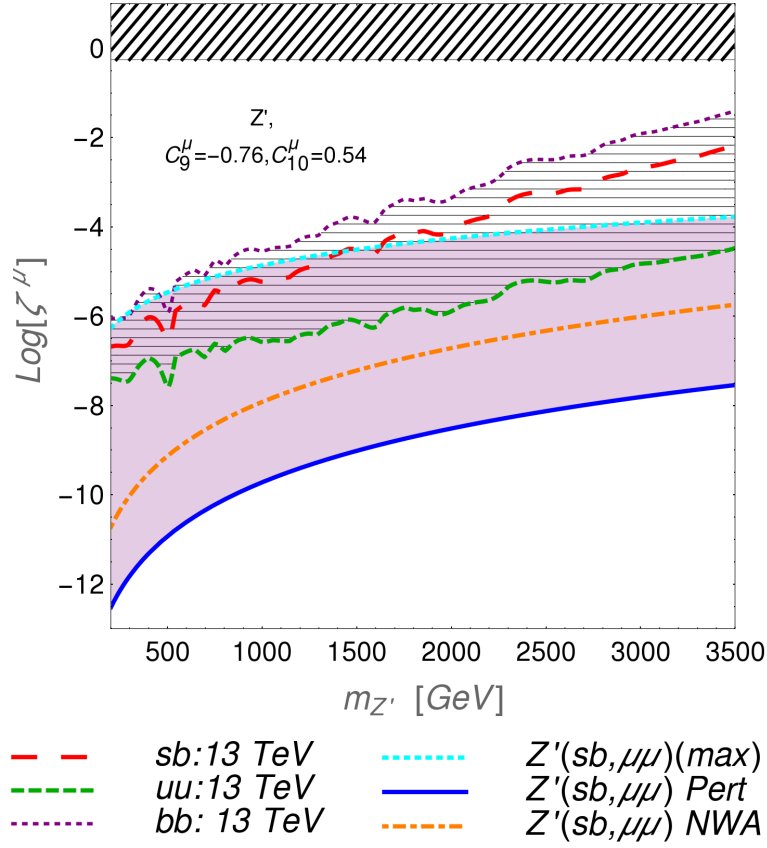


FIG. 5: Constraints on the general Z' boson that couples to all fermions. The pink shaded region reproduced from Fig. 3 (see text for discussion of how this region shifts for a general Z') shows where ζ^μ is small enough (below light-blue dashed line) to explain the R_K and R_{K^*} anomalies and also large enough (above blue solid line) to keep the Z' boson's couplings perturbative. Above the orange line, the Z' would be narrow. The upper bounds on ζ^μ derived from the 13 TeV ATLAS dilepton limits [64–66] for production via sb (red large-dashed), uu (green dashed), and bb (purple dotted) initial states are shown for comparison.

- There is a theoretical lower limit on ζ^μ imposed by perturbativity requirements on the Z' coupling to fermions; it is described by Eq. 26 and Eq. 42 and is presented in solid blue lines in the figures. This is a strict lower limit if the theory is to be self-consistent.
- The narrow width approximation imposes a somewhat softer lower limit on ζ^μ if we take $\Gamma/m_{Z'} \leq 0.1$. We chose to impose this limit to make sure that interference effects between BSM physics and the SM can be neglected; however the precise definition of what is deemed “narrow” can potentially vary from the value of 0.1. This limit is presented in pink dashed lines in all the plots.
- In Figs. 3 and 5, the region below the light blue dotted line is consistent with having the Z' boson explain the R_K anomalies observed by LHCb. Combining this with the above two constraints defines the pink shaded region as the region of interesting parameter space for our investigations.
- Some important constraints originate from LHC searches for new resonances decaying to dileptons. Limits on the cross-section for a narrow dimuon resonance imply upper bounds on ζ^μ which depend on the partonic production mechanism. These limits are displayed as diagonal lines in Figs. 3 and 5. In Fig. 3, where only production through sb annihilation is considered, the resulting upper bounds are just beginning to be sensitive to the region which can explain the R_K anomalies. In Fig. 5 we illustrate the dimuon bounds in the cases of production through $b\bar{b}$ and $u\bar{u}$ annihilation as well. In the case of production through $b\bar{b}$ annihilation, the

constraints are weakened due to the very low $b\bar{b}$ partonic luminosity. In the case of production through $u\bar{u}$ annihilation instead, however, substantial portions of the parameter space which can explain the R_K anomalies are now being probed.

- In general, as illustrated in Fig. 4 for the case of the minimal model produced through sb annihilation, direct LHC dijet resonance search constraints are weak. Instead, constraints on the dilepton searches, indirectly through the requirements of giving rise the R_K anomalies, can restrict portions of that dijet resonance parameter space.
- Finally, we illustrate in the general model that, if the number of production modes is increased, then the upper bound on the viable parameter space becomes stronger, because the maximum allowed value of ζ^μ is reduced. On the other hand, if the variety of decay modes is increased, then this upper bound becomes weaker. The perturbativity-derived lower bound on ζ^μ in the general model is always weaker than that in the minimal case; the lower bound corresponding to keeping the Z' narrow is always tightened.

VIII. CONCLUSION

In this work we consider the potential of a Z' boson to explain the recently observed R_K and R_{K^*} anomalies, and to still be consistent with latest ATLAS and CMS dijet and dilepton results. To this end, we consider two simple phenomenological models and work in the language of simplified limits. We first considered the minimal model needed to explain the anomalies, namely a Z' coupling only to bottom and strange quarks and to muons. However we expect that in a real (UV complete) theory, the Z' should couple to all the quarks and leptons, and therefore we also considered the constraints in a more general framework. For both cases we observe that the 13 TeV ATLAS and CMS dilepton results are beginning to constrain certain parts of the parameter space. Combining theoretical considerations with ATLAS and CMS results thus allows us to paint a picture on to which any UV complete theory with an extra Z' model can be mapped. We expect that with the next run of LHCb, which can potentially provide further clues to these flavor anomalies, and with the analysis of more ATLAS and CMS data on dijet and dilepton resonance searches, the allowed region will be further constrained – or, possibly, a new resonance will be discovered. In either case, the language of simplified limits can narrow down the interesting region of parameter space consistent with LHC results.

Acknowledgments

This material is based upon work supported, in part, by the National Science Foundation under Grant Nos. PHY-1519045 (R.S.C., K.M., D.S., and E.H.S.), and PHY-1417326 (J.I.). The authors would like to thank Jim Cline, for pointing out a typographic error in one of the equations in this manuscript; our correcting this error yielded significantly stronger constraints on the viable parameter space.

Appendix A: Expressions for the decay width

In this appendix, we present the expression for the partial decay widths of the Z' (to quarks) used in this paper. For a Z' coupled to a pair of quarks, we have,

$$\Gamma(Z' \rightarrow \bar{q}'q + \bar{q}q') = \nu\beta_{Z'}^2 \frac{\left(|c_L^{qq'}|^2 + |c_R^{qq'}|^2\right) m_{Z'}}{8\pi} . \quad (\text{A1})$$

Here $\nu = 1/2$ if $q = q'$ and $\nu = 1$ if $q \neq q'$.

$$\Gamma(Z' \rightarrow \bar{t}q + \bar{q}t) = \beta_{Z'}^2 \frac{(|c_L^{tq}|^2 + |c_R^{tq}|^2) m_{Z'}}{8\pi} (1-x)^2 (2+x) . \quad (\text{A2})$$

Here $x = m_t^2/m_{Z'}^2$.

$$\Gamma(Z' \rightarrow \bar{t}t) = \beta_{Z'}^2 \frac{|c_L^{tt}|^2 + |c_R^{tt}|^2 + (|c_L^{tt}|^2 + |c_R^{tt}|^2 - 6c_L^{tt}c_R^{tt})x}{8\pi} \cdot m_{Z'} \sqrt{1-4x} . \quad (\text{A3})$$

We have neglected mass effects of the top to simplify our discussion. Introducing masses will only reduce the partial width to top final states. Finally for leptons we have

$$\Gamma(Z' \rightarrow \bar{l}l) = \beta_{Z'}^2 \frac{(|c_V^{\mu}|^2 + |c_A^{\mu}|^2) m_{Z'}}{12\pi} . \quad (\text{A4})$$

-
- [1] **Heavy Flavor Averaging Group** Collaboration, Y. Amhis *et al.*, “Averages of b -hadron, c -hadron, and τ -lepton properties as of summer 2014,” [arXiv:1412.7515 \[hep-ex\]](#).
- [2] “Talk by Simone Bifani for the LHCb collaboration, CERN, 18/4/2016,”. <https://indico.cern.ch/event/580620/>. Accessed: 2017-04-18.
- [3] **LHCb** Collaboration, R. Aaij *et al.*, “Test of lepton universality using $B^+ \rightarrow K^+ \ell^+ \ell^-$ decays,” [Phys. Rev. Lett. **113** \(2014\) 151601](#), [arXiv:1406.6482 \[hep-ex\]](#).
- [4] W. Altmannshofer, P. Stangl, and D. M. Straub, “Interpreting Hints for Lepton Flavor Universality Violation,” [arXiv:1704.05435 \[hep-ph\]](#).
- [5] A. K. Alok, D. Kumar, J. Kumar, and R. Sharma, “Lepton flavor non-universality in the B-sector: a global analyses of various new physics models,” [arXiv:1704.07347 \[hep-ph\]](#).
- [6] B. Capdevila, A. Crivellin, S. Descotes-Genon, J. Matias, and J. Virto, “Patterns of New Physics in $b \rightarrow s \ell^+ \ell^-$ transitions in the light of recent data,” [arXiv:1704.05340 \[hep-ph\]](#).
- [7] G. D’Amico, M. Nardecchia, P. Panci, F. Sannino, A. Strumia, R. Torre, and A. Urbano, “Flavour anomalies after the R_{K^*} measurement,” [arXiv:1704.05438 \[hep-ph\]](#).
- [8] L.-S. Geng, B. Grinstein, S. Jäger, J. Martin Camalich, X.-L. Ren, and R.-X. Shi, “Towards the discovery of new physics with lepton-universality ratios of $b \rightarrow s \ell \ell$ decays,” [arXiv:1704.05446 \[hep-ph\]](#).
- [9] M. Ciuchini, A. M. Coutinho, M. Fedele, E. Franco, A. Paul, L. Silvestrini, and M. Valli, “On Flavourful Easter eggs for New Physics hunger and Lepton Flavour Universality violation,” [arXiv:1704.05447 \[hep-ph\]](#).
- [10] G. Hiller and I. Nisandzic, “ R_K and R_{K^*} beyond the Standard Model,” [arXiv:1704.05444 \[hep-ph\]](#).
- [11] A. K. Alok, B. Bhattacharya, A. Datta, D. Kumar, J. Kumar, and D. London, “New Physics in $b \rightarrow s \mu^+ \mu^-$ after the Measurement of R_{K^*} ,” [arXiv:1704.07397 \[hep-ph\]](#).
- [12] A. Celis, J. Fuentes-Martin, A. Vicente, and J. Virto, “Gauge-invariant implications of the LHCb measurements on Lepton-Flavour Non-Universality,” [arXiv:1704.05672 \[hep-ph\]](#).
- [13] D. Ghosh, “Explaining the R_K and R_{K^*} anomalies,” [arXiv:1704.06240 \[hep-ph\]](#).
- [14] D. Bardhan, P. Byakti, and D. Ghosh, “Role of Tensor operators in R_K and R_{K^*} ,” [arXiv:1705.09305 \[hep-ph\]](#).
- [15] G. Bélanger, C. Delaunay, and S. Westhoff, “A Dark Matter Relic From Muon Anomalies,” [Phys. Rev. **D92** \(2015\) 055021](#), [arXiv:1507.06660 \[hep-ph\]](#).
- [16] J. F. Kamenik, Y. Soreq, and J. Zupan, “Lepton flavor universality violation without new sources of quark flavor violation,” [arXiv:1704.06005 \[hep-ph\]](#).
- [17] C.-W. Chiang, X.-G. He, J. Tandean, and X.-B. Yuan, “ $R_{K^{(*)}}$ and related $b \rightarrow s \ell \bar{\ell}$ anomalies in minimal flavor violation framework with Z' boson,” [arXiv:1706.02696 \[hep-ph\]](#).
- [18] I. Garcia Garcia, “LHCb anomalies from a natural perspective,” [JHEP **03** \(2017\) 040](#), [arXiv:1611.03507 \[hep-ph\]](#).
- [19] W. Altmannshofer, S. Gori, S. Profumo, and F. S. Queiroz, “Explaining dark matter and B decay anomalies with an $L_\mu - L_\tau$ model,” [JHEP **12** \(2016\) 106](#), [arXiv:1609.04026 \[hep-ph\]](#).
- [20] B. Allanach, F. S. Queiroz, A. Strumia, and S. Sun, “Z models for the LHCb and $g - 2$ muon anomalies,” [Phys. Rev. **D93** no. 5, \(2016\) 055045](#), [arXiv:1511.07447 \[hep-ph\]](#). [Erratum: *Phys. Rev. D* **95**, no. 11, 119902 (2017)].

- [21] A. Crivellin, G. D'Ambrosio, and J. Heeck, “Explaining $h \rightarrow \mu^\pm \tau^\mp$, $B \rightarrow K^* \mu^+ \mu^-$ and $B \rightarrow K \mu^+ \mu^- / B \rightarrow K e^+ e^-$ in a two-Higgs-doublet model with gauged $L_\mu - L_\tau$,” *Phys. Rev. Lett.* **114** (2015) 151801, [arXiv:1501.00993 \[hep-ph\]](#).
- [22] A. Crivellin, L. Hofer, J. Matias, U. Nierste, S. Pokorski, and J. Rosiek, “Lepton-flavour violating B decays in generic Z' models,” *Phys. Rev.* **D92** no. 5, (2015) 054013, [arXiv:1504.07928 \[hep-ph\]](#).
- [23] A. Crivellin, J. Fuentes-Martin, A. Greljo, and G. Isidori, “Lepton Flavor Non-Universality in B decays from Dynamical Yukawas,” *Phys. Lett.* **B766** (2017) 77–85, [arXiv:1611.02703 \[hep-ph\]](#).
- [24] S. L. Glashow, D. Guadagnoli, and K. Lane, “Lepton Flavor Violation in B Decays?,” *Phys. Rev. Lett.* **114** (2015) 091801, [arXiv:1411.0565 \[hep-ph\]](#).
- [25] B. Bhattacharya, A. Datta, D. London, and S. Shivashankara, “Simultaneous Explanation of the R_K and $R(D^{(*)})$ Puzzles,” *Phys. Lett.* **B742** (2015) 370–374, [arXiv:1412.7164 \[hep-ph\]](#).
- [26] B. Bhattacharya, A. Datta, J.-P. Gu  vin, D. London, and R. Watanabe, “Simultaneous Explanation of the R_K and $R_{D^{(*)}}$ Puzzles: a Model Analysis,” *JHEP* **01** (2017) 015, [arXiv:1609.09078 \[hep-ph\]](#).
- [27] D. Be  re  vi   and O. Sumensari, “A leptoquark model to accommodate $R_K^{\text{exp}} < R_K^{\text{SM}}$ and $R_{K^*}^{\text{exp}} < R_{K^*}^{\text{SM}}$,” [arXiv:1704.05835 \[hep-ph\]](#).
- [28] Y. Cai, J. Gargalionis, M. A. Schmidt, and R. R. Volkas, “Reconsidering the One Leptoquark solution: flavor anomalies and neutrino mass,” [arXiv:1704.05849 \[hep-ph\]](#).
- [29] S. Di Chiara, A. Fowlie, S. Fraser, C. Marzo, L. Marzola, M. Raidal, and C. Spethmann, “Minimal flavor-changing Z' models and muon $g - 2$ after the R_{K^*} measurement,” [arXiv:1704.06200 \[hep-ph\]](#).
- [30] R. Alonso, P. Cox, C. Han, and T. T. Yanagida, “Anomaly-free local horizontal symmetry and anomaly-full rare B -decays,” [arXiv:1704.08158 \[hep-ph\]](#).
- [31] C. Bonilla, T. Modak, R. Srivastava, and J. W. F. Valle, “ $U(1)_{B_3-3L_\mu}$ gauge symmetry as the simplest description of $b \rightarrow s$ anomalies,” [arXiv:1705.00915 \[hep-ph\]](#).
- [32] J. Ellis, M. Fairbairn, and P. Tunney, “Anomaly-Free Models for Flavour Anomalies,” [arXiv:1705.03447 \[hep-ph\]](#).
- [33] F. Bishara, U. Haisch, and P. F. Monni, “On Light Resonance Interpretations of the B Decay Anomalies,” [arXiv:1705.03465 \[hep-ph\]](#).
- [34] Y. Tang and Y.-L. Wu, “Flavor Non-universality Gauge Interactions and Anomalies in B -Meson Decays,” [arXiv:1705.05643 \[hep-ph\]](#).
- [35] “Talk by Antonio Romero Vidal for the LHCb collabortion,”. <https://indico.cern.ch/event/632397/>. Accessed: 2017-04-18.
- [36] R. S. Chivukula, P. Ittisamai, K. Mohan, and E. H. Simmons, “Simplified Limits on Resonances at the LHC,” *Phys. Rev.* **D94** no. 9, (2016) 094029, [arXiv:1607.05525 \[hep-ph\]](#).
- [37] **LHCb** Collaboration, R. Aaij et al., “Test of lepton universality using $B^+ \rightarrow K^+ \ell^+ \ell^-$ decays,” *Phys. Rev. Lett.* **113** (2014) 151601, [arXiv:1406.6482 \[hep-ex\]](#).
- [38] G. Hiller and F. Kruger, “More model-independent analysis of $b \rightarrow s$ processes,” *Phys. Rev.* **D69** (2004) 074020, [arXiv:hep-ph/0310219 \[hep-ph\]](#).
- [39] M. Bordone, G. Isidori, and A. Pattori, “On the Standard Model predictions for R_K and R_{K^*} ,” *Eur. Phys. J.* **C76** no. 8, (2016) 440, [arXiv:1605.07633 \[hep-ph\]](#).
- [40] **LHCb** Collaboration, R. Aaij et al., “Measurement of Form-Factor-Independent Observables in the Decay $B^0 \rightarrow K^{*0} \mu^+ \mu^-$,” *Phys. Rev. Lett.* **111** (2013) 191801, [arXiv:1308.1707 \[hep-ex\]](#).
- [41] **LHCb** Collaboration, R. Aaij et al., “Angular analysis of the $B^0 \rightarrow K^{*0} \mu^+ \mu^-$ decay using 3 fb^{-1} of integrated luminosity,” *JHEP* **02** (2016) 104, [arXiv:1512.04442 \[hep-ex\]](#).
- [42] **Belle** Collaboration, S. Wehle et al., “Lepton-Flavor-Dependent Angular Analysis of $B \rightarrow K^* \ell^+ \ell^-$,” *Phys. Rev. Lett.* **118** no. 11, (2017) 111801, [arXiv:1612.05014 \[hep-ex\]](#).
- [43] F. Beaujean, C. Bobeth, and D. van Dyk, “Comprehensive Bayesian analysis of rare (semi)leptonic and radiative B decays,” *Eur. Phys. J.* **C74** (2014) 2897, [arXiv:1310.2478 \[hep-ph\]](#). [Erratum: *Eur. Phys. J.* **C74**, 3179(2014)].
- [44] S. Descotes-Genon, L. Hofer, J. Matias, and J. Virto, “Global analysis of $b \rightarrow s \ell \ell$ anomalies,” *JHEP* **06** (2016) 092, [arXiv:1510.04239 \[hep-ph\]](#).
- [45] T. Hurth, F. Mahmoudi, and S. Neshatpour, “On the anomalies in the latest LHCb data,” *Nucl. Phys.* **B909** (2016) 737–777, [arXiv:1603.00865 \[hep-ph\]](#).
- [46] W. Altmannshofer, C. Niehoff, P. Stangl, and D. M. Straub, “Status of the $B \rightarrow K^* \mu^+ \mu^-$ anomaly after Moriond 2017,” [arXiv:1703.09189 \[hep-ph\]](#).
- [47] M. Beneke, T. Feldmann, and D. Seidel, “Systematic approach to exclusive $B \rightarrow V l^+ l^-$, $V \gamma$ decays,” *Nucl. Phys.* **B612** (2001) 25–58, [arXiv:hep-ph/0106067 \[hep-ph\]](#).

- [48] B. Grinstein and D. Pirjol, “Exclusive rare $B \rightarrow K^* \ell^+ \ell^-$ decays at low recoil: Controlling the long-distance effects,” *Phys. Rev.* **D70** (2004) 114005, [arXiv:hep-ph/0404250 \[hep-ph\]](#).
- [49] U. Egede, T. Hurth, J. Matias, M. Ramon, and W. Reece, “New observables in the decay mode $\bar{B}_d \rightarrow \bar{K}^{*0} l^+ l^-$,” *JHEP* **11** (2008) 032, [arXiv:0807.2589 \[hep-ph\]](#).
- [50] A. Khodjamirian, T. Mannel, A. A. Pivovarov, and Y. M. Wang, “Charm-loop effect in $B \rightarrow K^{(*)} \ell^+ \ell^-$ and $B \rightarrow K^* \gamma$,” *JHEP* **09** (2010) 089, [arXiv:1006.4945 \[hep-ph\]](#).
- [51] M. Beylich, G. Buchalla, and T. Feldmann, “Theory of $B \rightarrow K^{(*)} \ell^+ \ell^-$ decays at high q^2 : OPE and quark-hadron duality,” *Eur. Phys. J.* **C71** (2011) 1635, [arXiv:1101.5118 \[hep-ph\]](#).
- [52] A. Khodjamirian, T. Mannel, and Y. M. Wang, “ $B \rightarrow K \ell^+ \ell^-$ decay at large hadronic recoil,” *JHEP* **02** (2013) 010, [arXiv:1211.0234 \[hep-ph\]](#).
- [53] S. Jäger and J. Martin Camalich, “On $B \rightarrow V \ell \ell$ at small dilepton invariant mass, power corrections, and new physics,” *JHEP* **05** (2013) 043, [arXiv:1212.2263 \[hep-ph\]](#).
- [54] R. R. Horgan, Z. Liu, S. Meinel, and M. Wingate, “Calculation of $B^0 \rightarrow K^{*0} \mu^+ \mu^-$ and $B_s^0 \rightarrow \phi \mu^+ \mu^-$ observables using form factors from lattice QCD,” *Phys. Rev. Lett.* **112** (2014) 212003, [arXiv:1310.3887 \[hep-ph\]](#).
- [55] J. Lyon and R. Zwicky, “Resonances gone topsy turvy - the charm of QCD or new physics in $b \rightarrow s \ell^+ \ell^-$,” [arXiv:1406.0566 \[hep-ph\]](#).
- [56] S. Descotes-Genon, L. Hofer, J. Matias, and J. Virto, “On the impact of power corrections in the prediction of $B \rightarrow K^* \mu^+ \mu^-$ observables,” *JHEP* **12** (2014) 125, [arXiv:1407.8526 \[hep-ph\]](#).
- [57] S. Jäger and J. Martin Camalich, “Reassessing the discovery potential of the $B \rightarrow K^* \ell^+ \ell^-$ decays in the large-recoil region: SM challenges and BSM opportunities,” *Phys. Rev.* **D93** no. 1, (2016) 014028, [arXiv:1412.3183 \[hep-ph\]](#).
- [58] A. Bharucha, D. M. Straub, and R. Zwicky, “ $B \rightarrow V \ell^+ \ell^-$ in the Standard Model from light-cone sum rules,” *JHEP* **08** (2016) 098, [arXiv:1503.05534 \[hep-ph\]](#).
- [59] B. Capdevila, S. Descotes-Genon, L. Hofer, and J. Matias, “Hadronic uncertainties in $B \rightarrow K^* \mu^+ \mu^-$: a state-of-the-art analysis,” *JHEP* **04** (2017) 016, [arXiv:1701.08672 \[hep-ph\]](#).
- [60] V. G. Chobanova, T. Hurth, F. Mahmoudi, D. Martinez Santos, and S. Neshatpour, “Large hadronic power corrections or new physics in the rare decay $B \rightarrow K^* \ell \ell$,” [arXiv:1702.02234 \[hep-ph\]](#).
- [61] J. Pumplin, D. R. Stump, J. Huston, H. L. Lai, P. M. Nadolsky, and W. K. Tung, “New generation of parton distributions with uncertainties from global QCD analysis,” *JHEP* **07** (2002) 012, [arXiv:hep-ph/0201195 \[hep-ph\]](#).
- [62] A. Greljo and D. Marzocca, “High- p_T dilepton tails and flavour physics,” [arXiv:1704.09015 \[hep-ph\]](#).
- [63] A. K. Alok, B. Bhattacharya, D. Kumar, J. Kumar, D. London, and S. U. Sankar, “New physics in $b \rightarrow s \mu^+ \mu^-$: Distinguishing models through CP-violating effects,” *Phys. Rev.* **D96** no. 1, (2017) 015034, [arXiv:1703.09247 \[hep-ph\]](#).
- [64] **ATLAS Collaboration**, G. Aad et al., “Search for contact interactions and large extra dimensions in the dilepton channel using proton-proton collisions at $\sqrt{s} = 8$ TeV with the ATLAS detector,” *Eur. Phys. J.* **C74** no. 12, (2014) 3134, [arXiv:1407.2410 \[hep-ex\]](#).
- [65] **ATLAS Collaboration**, G. Aad et al., “Search for high-mass dilepton resonances in pp collisions at $\sqrt{s} = 8$ TeV with the ATLAS detector,” *Phys. Rev.* **D90** no. 5, (2014) 052005, [arXiv:1405.4123 \[hep-ex\]](#).
- [66] **ATLAS Collaboration**, “Search for new high-mass phenomena in the dilepton final state using 36.1 fb $^{-1}$ of proton-proton collision data at $\sqrt{s} = 13$ TeV with the ATLAS detector,” Tech. Rep. ATLAS-CONF-2017-027, CERN, Geneva, Apr, 2017. <http://cds.cern.ch/record/2259039>.
- [67] **ATLAS Collaboration**, G. Aad et al., “Measurement of the double-differential high-mass Drell-Yan cross section in pp collisions at $\sqrt{s} = 8$ TeV with the ATLAS detector,” *JHEP* **08** (2016) 009, [arXiv:1606.01736 \[hep-ex\]](#).
- [68] **CMS Collaboration**, “Searches for dijet resonances in pp collisions at $\sqrt{s} = 13$ TeV using data collected in 2016,” Tech. Rep. CMS-PAS-EXO-16-056, CERN, Geneva, 2017. <https://cds.cern.ch/record/2256873>.
- [69] **ATLAS Collaboration**, M. Aaboud et al., “Search for new phenomena in dijet events using 37 fb $^{-1}$ of pp collision data collected at $\sqrt{s} = 13$ TeV with the ATLAS detector,” [arXiv:1703.09127 \[hep-ex\]](#).
- [70] **ATLAS Collaboration**, G. Aad et al., “Search for new phenomena in the dijet mass distribution using pp collision data at $\sqrt{s} = 8$ TeV with the ATLAS detector,” *Phys. Rev.* **D91** no. 5, (2015) 052007, [arXiv:1407.1376 \[hep-ex\]](#).